

Bidirectional Reflectance Measurements of Meteorites Acquired by FGI's Field Goniospectrometer

Maria Gritsevich ^{1,2,3}, Teemu Hakala ¹, Jouni Peltoniemi ¹, Mark Paton ⁴, Jarkko Stenman ⁵, and Arto Luttinen ⁵

(1) Department of Remote Sensing and Photogrammetry, Finnish Geodetic Institute, (2) Department of Physics, University of Helsinki, (3) Institute of Mechanics and Faculty of Mechanics and Mathematics, Lomonosov Moscow State University, (4) Finnish Meteorological Institute, (5) Finnish Museum of Natural History, University of Helsinki

Abstract. Meteorite studies represent a low-cost opportunity for probing the cosmic matter that reaches the Earth's surface and for revealing the origin of our Solar system. In addition they complement results of sample-return missions that bring back pristine samples of this material. The main difficulty, however, with interpreting meteorite records is that, apart from a few exceptional cases, we do not know their exact origin i.e. the parent body a particular sample is coming from. In the present study we provide results of multiangular bidirectional reflectance measurements of relatively big meteorite samples, from the Finnish Museum of Natural History, using the field goniospectrometer FIGIFIGO. We discuss possible matches between our measured reflectance spectra of meteorites with the reflectance spectra of asteroids. We discuss the features in the spectra and their relationship to the physical properties of the sample/asteroid.

Introduction

Understanding the nature and origin of meteoroids that pass by the Earth and occasionally hit our planet help us to predict and be prepared for possible future Near Earth Objects (NEO) impact threats. In terms of orbital elements, NEOs are asteroids and comets with perihelion distance q less than 1.3 AU (<http://neo.jpl.nasa.gov/neo.html>). Near-Earth Comets (NECs) are further restricted to include only short-period comets with orbital period P less than 200 years. The majority of NEOs are asteroids, referred to as Near-Earth Asteroids (NEAs). Thus a number of recent studies are addressing the problem of matching meteorites to their asteroid origin based on evaluated orbits, or, when there are no good observations available for orbital parameters derivation, on the basis of their mineral composition [1-3].

It is problematic to compare the meteorite and asteroid groups directly, as the meteorite collection is subject to strong selection effects. Firstly the strength of meteorites controls those that survive entry into the atmosphere [4]. It is thought there is also a selection effect due to size. Smaller meteorites are more easily transported out of the main belt due to the Yarkovsky Effect [1] than the large NEAs. These in turn are from a few locations near resonant orbits with Jupiter. It is also thought that meteorites sample the inner main belt [5] although it is possible that meteorites can travel from further out [6]. The metamorphic evolution of asteroids is preserved within the meteorite collection and can give us information on differentiated asteroids such as Vesta as with the HED group of meteorites [7]. Some good matches have been made between individual meteorite spectra and NEA [8] as well as between meteorite spectra and large main belt asteroids [9]. The principle properties of the spectra used to identify possible matches between meteorites and asteroids are the band minimum location and Band Area Ratio. The band minimum is the wavelength location of an absorption band in the spectra. The BAR is the ratio between the area of the bands in the spectra. These properties are diagnostic of the object's mineralogy and to lesser extend other physical properties such as their surface roughness and grain size e.g. [10].

The spectra of meteorites and asteroids are also dependent on observational conditions such as the phase angle between the line connecting the light source (e.g. sun) with the target and the line connecting the target with the observer (Fig. 1). This is a key effect that needs to be understood, to help improve matches between meteorites and asteroids, as this phase angle, when observing asteroids, varies due to the changing orbital positions of the target and viewer. Variations in the band depths, band minimum locations, the band area ratio and spectral slope have been noted to vary with phase angle and have been characterised [11]. Although this effect does not seem to affect the mineralogical analysis very much it is important for understanding optical effects and their relationship to the physical properties such as surface roughness and grain size.

What is BRF?

The reflectance property of a surface is described by its bidirectional reflectance factor (BRF). BRF is defined as a ratio of the reflected light intensity of a given target to an ideal Lambertian reflector with a spherical albedo of 1.0 under same incident irradiation:

$$R(\mu, \mu_0, \phi, \phi_0) = \frac{\pi I(\mu, \phi)}{\mu_0 F_0(\mu_0, \phi_0)}$$

where F_0 is the incident collimated flux and I is reflected radiance. The definition of angles is given on Fig. 1. Albedo, or reflection coefficient, is defined as a ratio of all reflected (scattered) radiation to all incident radiation. Being a dimensionless fraction, albedo may also be expressed as a percentage, and it is measured on a scale from zero for no reflecting power of a perfectly black body, to 1 for perfect reflection of a white surface. Depending on application, there are many variations of the definition of the albedo, and thus one needs to be careful applying formulae from another field. The albedo is a function of the incident light distribution and it is related to BRF as

$$A = \frac{\int d\lambda \int d\phi \int d\mu \int d\phi_0 \int d\mu_0 R(\mu, \phi, \mu_0, \phi_0, \lambda) I_0(\mu_0, \phi_0, \lambda)}{\int d\lambda \int d\phi \int d\mu \int d\phi_0 \int d\mu_0 I_0(\mu_0, \phi_0, \lambda)}$$

BRFs of typical remote sensing targets vary by a large scale. Some targets are forward scatterers, some are backscatterers, some have a strong specular reflection, some reflect highly to low zenith angles [12-15]. Each target has its unique BRF that depends on all of its geometrical and physical properties. Thus exploitation of BRF information is a valuable tool in target classification and quantification.

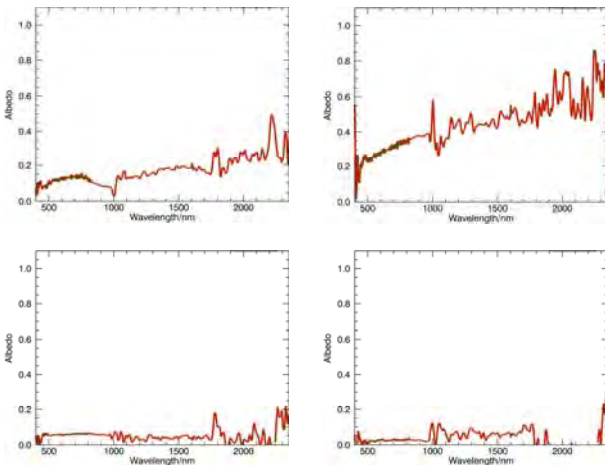


Fig. 2. Examples of measured albedo: Bruderheim, meteorite: cut (upper picture on the left) and rough surface (on the left, down), Canyon Diablo meteorite, rough side (on the right, up), Charcas meteorite, rough side (on the right, down)

Summary of selected meteorite samples

The summary of the meteorite samples selected for our measurements from the Finnish Museum of Natural History (Geological museum) is presented in the table below. The meteorite exhibition belongs to the Geological museum and it is on display at the Mineral Cabinet in association with the Helsinki University museum *

Name	Observed fall?	Year found	Country	Classification	Total Mass found
Bruderheim	March 4, 1960	1960	Canada	L6	303 kg
Canyon Diablo	No	1891	United States	Iron, IAB-MG	30 MT
Cape York	No	1818	Greenland	Iron, IIIAB	58.2 MT
Charcas	No	1804	Mexico	Iron, IIIAB	1.4 MT
Gibeon	No	1836	Namibia	Iron, IVA	26 MT
Marjalahiti	June 1, 1902	1902	Russia	Pallasite, PMG	45 kg

* <http://www.luomus.fi/english/exhibitions/mineralcabinet/index.htm/>

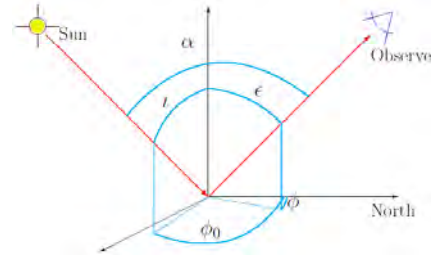


Fig. 1. Definition of the angles used in surface reflectance work: ϵ and μ are the zenith angles of the emergent (Observer) and incident (solar) radiation respectively (shorthands $\mu = \cos \epsilon$ and $\mu_0 = \cos \mu_0$ are also used), ϕ and ϕ_0 are the corresponding azimuths.

The phase or back scattering angle α is the angle between the Observer and the Sun. The principal plane is fixed by the solar direction and the surface normal, while the cross plane is a vertical plane perpendicular to the principal plane.

Instrumentation

The meteorite BRF measurements have been taken using the Finnish Geodetic Institute Field Goniospectrometer FIGIFIGO, an automated portable instrument for multiangular reflectance measurements (Fig.3). The FIGIFIGO system consists of a motor-driven moving arm that tilts up to 90° from the vertical, fore optics in the high end of the arm, and an ASD FieldSpec Pro FR 350-2500 nm spectroradiometer. Accurate zenith angles are read with an inclinometer. The detailed description of the instrument can be found in [16]. Typically, the footprint diameter is about 10 cm, elongating at larger sensor zenith angles as $1/\cos \theta$, and wandering around a few centimetres by bending and with azimuthal movements. A motorised fine tune mirror is installed to correct paraxial and bending errors and to keep the measurement point stable to an accuracy of 2 mm. The instrument has been calibrated by taking a nadir measurement from a Labsphere Spectralon white reference plate before and after each sequence. The Spectralon has been carefully levelled at horizontal with a bubble level with an accuracy of about 1°. All the measurements were taken from 0° relative azimuth (principal plane). Due to the small target size, the zenith angles were restricted to $\pm 60^\circ$. The measurement arm was first driven to maximum angle and then slowly to minimum angle, while continuously collecting spectra. The instrument was calibrated by taking a nadir measurement from a Labsphere Spectralon white reference plate before and after each sequence. The Spectralon has been carefully levelled at horizontal with a bubble level with an accuracy of about 1°. The accuracy of the spectral BRF measurements using FIGIFIGO is estimated to be 2-3% in the visible band and good conditions, with a polarisation accuracy of 2-5%. Angle registration accuracy is 2°.

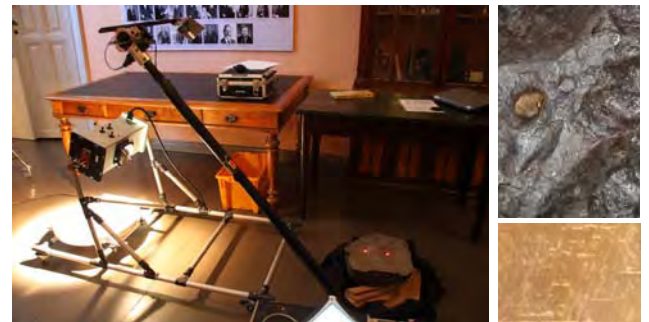


Fig. 3. The FIGIFIGO measuring BRDF of selected sample Gibeon (left). The active optics system is located horizontally at the top of the measuring arm, and is looking down at the target through a mirror. FIGIFIGO consists of the following main components: casing, measurement arm, rugged computer, and a sunphotometer on a tripod. The casing contains the main sensor ASD FieldSpec Pro FR optical fiber spectroradiometer (350 – 2500 nm), most of the electronics, and batteries. On the right: ablated (rough) and cut Gibeon surfaces.

Preliminary results and conclusions

The results of our measurements are partly presented on Fig. 4 for the L6 chondrite, Bruderheim. The spectra are obtained at different zenith angles. These show a general reddening of the spectra as the absolute zenith angle increases. For a non-rough surface of the L6 chondrite Bruderheim the spectral slope increases with decreasing (i.e. more negative) zenith angle. The absolute value of the zenith angle in the principal plane may be thought as analogous to phase angle.

This then follows a similar trend found previously [12], where the spectral slope gradient for various chondrites (including L6) was found to increase significantly with increasing phase angle. The spectral slope gradient is known to increase with phase angle for S-type asteroids [17] which are linked to ordinary chondrites. Similar trends of increasing slope with decreasing zenith angles has not been observed for the iron meteorites. We have observed the spurious variations in the spectra for Bruderheim meteorite especially around 0.9 and 1.8 microns. That absorption bands have to be expected in these regions for L6 meteorite types. MG, TH and JP acknowledge financial support provided by the Academy of Finland. We would like to thank Dr. Pierre Vernazza (ESO & Laboratoire d'Astrophysique de Marseille) for his interest to conducted measurements and fruitful discussion on the obtained results.

Fig. 4. Spectra from the Bruderheim for a variety of zenith angles in the principal plane.

[1] Vernazza, P., Binzel, R.P., Thomas, C.A., DeMeo, F.E., Bus, S.J., Rivkin, A.S., Tokunaga, A.T. Compositional differences between meteorites and near-Earth asteroids // Nature 454 (7206), pp. 858-860, 2008.
 [2] Bland, P.A., Spurný, P., Townes, M.C., Bevan, A.W.R., Singleton, A.T., Botke Jr., W.F., Greenwood, R.C., Chesley, S.R., Sierbeny, L., Borovicka, J., Cepelcha, Z., McClafferty, T.P., Vaughan, D., Benedi, G.K., Deacon, G., Howard, K.T., Franchi, L.A., Hough, R.M. An anomalous basaltic meteorite from the innermost main belt // Science 325 (5947), pp. 1525-1527, 2009.
 [3] Binzel, R.P., Morbidelli, A., Merosane, S., Demeo, F.E., Birilan, M., Vernazza, P., Thomas, C.A., Rivkin, A.S., Bus, S.J., Tokunaga, A.T. Earth encounters as the origin of fresh surfaces on near-Earth asteroids // Nature 463 (7279), pp. 331-334, 2010.
 [4] Cepelcha, Z., Spurný, P., Borovicka, J., Kecklová, J. Atmospheric fragmentation of meteoroids // Astronomy & Astrophysics, 279, pp. 615-626, 1993.
 [5] Botke Jr., W.F., Wokoschick, D., Rubincam, D.P., Broz, M.J. The effect of Yarkovsky thermal forces on the dynamical evolution of asteroids and meteoroids // In: Botke, W.F., Cellino, A., Paolucci, P., Binzel, R.P. (Eds.), Asteroids III. Univ. of Arizona Press, Tucson, pp. 395-408, 2002.
 [6] Nesvorný, D., Wokoschick, D., Morbidelli, A., Botke, B.F. Asteroidal source of L chondrite meteorites // Icarus, 200, pp. 698-701, 2009.
 [7] McCord, T.B., Adams, J. B., Johnson, T. V. Asteroid Vesta: Spectral reflectivity and compositional implications // Science, 168, pp. 1445-1447, 1970.
 [8] McFadden, L.A., Gaffey, M.J., McCord, T.B. Near-Earth asteroids: Possible sources from reflectance spectroscopy // Science, 229, pp. 160-163, 1985.
 [9] Binzel, R.P., Xu, S., Chips off Asteroid 4 Vesta: Evidence for the parent body of basaltic achondrite meteorites // Science, 260, pp. 186-191, 1993.
 [10] Paton, M.D., Muinonen, K., Pesonen, L. J., Kuosmanen, V., Kohout, T., Laitinen, J., Lehtinen, M. A PCA study to determine how features in meteorite reflectance spectra vary with the samples' physical properties // Journal of Quantitative Spectroscopy & Radiative Transfer, 112, pp. 1804-1814, 2011.
 [11] Sanchez, J.A., Reddy, V., Nathaus, A., Choutis, E. A., Mann, P. and Hisinger, H. Phase reddening on near-Earth asteroids: Implications for mineralogical analysis, space weathering and taxonomic classification // Icarus, 202, pp. 36-50, 2012.
 [12] Peltoniemi, J.I. Spectropolarised ray-tracing simulations in densely packed particulate medium // Journal of Quantitative Spectroscopy and Radiative Transfer 108 (2), pp. 180-196, 2007.
 [13] Peltoniemi, J.I., Hakala, T., Saavalainen, J., Pattonen, E. Polarised bidirectional reflectance factor measurements from soil, stones, and snow // Journal of Quantitative Spectroscopy and Radiative Transfer 110(17), pp. 1940-1953, 2009.
 [14] Peltoniemi, J.I., Kaasalainen, S., Näränen, J., Matikainen, L., Piironen, J. Measurement of Directional and Spectral Signatures of Light Reflectance by Snow // IEEE Transactions on Geoscience and Remote Sensing 43(10), pp. 2294-2304, 2005.
 [15] Peltoniemi, J.I., Kaasalainen, S., Näränen, J., Rautiainen, M., Stenborg, P., Snelander, H., Snolander, S., Väipio, P. BRDF measurement of underson vegetation in pine forests: dwarf shrubs, lichen, and moss // Remote Sensing of Environment 94, pp. 343-354, 2005.
 [16] Hakala, T. Improvements, Calibration, and Accuracy of the Finnish Geodetic Institute Field Goniospectrometer // M.Sc. Thesis, Helsinki University of Technology, 2009.
 [17] Nathaus, A. A spectral study of the Eunomia asteroid family Part II: The small bodies // Icarus, 208, pp.252-275, 2010.